Different intracellular distribution of avian reovirus core protein sigmaA in cells of avian and mammalian origin

Lorena Vázquez-Iglesias, Irene Lostalé Seijo, José Martínez-Costas, Javier Benavente

Accepted Manuscript

How to cite:

Vázquez-Iglesias, L., Lostalé-Seijo, I., Martínez-Costas, J., & Benavente, J. (2012). Different intracellular distribution of avian reovirus core protein sigmaA in cells of avian and mammalian origin. Virology, 432(2), 495-504. doi: 10.1016/j.virol.2012.07.007

Different intracellular distribution of avian reovirus core protein sigmaA in cells of avian and mammalian origin

AUTHORS

Lorena Vázquez-Iglesias [a, 1], Irene Lostalé-Seijo [1], José Martínez-Costas and Javier Benavente*

AFFILIATION:

Departamento de Bioquímica y Biología Molecular, Facultad de Farmacia, y Centro Singular de Investigación en Química Biológica y Materiales Moleculares (CIQUS), Universidad de Santiago de Compostela, 15782-Santiago de Compostela, Spain

* Corresponding author: Javier Benavente

Edificio CIQUS, despacho D3.7, Campus Vida, Universidad de Santiago de Compostela, 15782- Santiago de Compostela, Spain

Phone: 34-881815734

Fax: 34-881815768

Email: franciscojavier.benavente@usc.es

[a] Current address: Departamento de Bioquímica, Genética e Inmunología, Facultad de Biología, Universidad de Vigo, 36310-Vigo (Pontevedra), Spain

[1] These authors contribute equally to this work.

Key words: avian reovirus; sigmaA; intracellular distribution; nuclear import; CRM1-dependent export; nuclear matrix; nucleocytoplasmic shuttling

Abstract

A comparative analysis of the intracellular distribution of avian reovirus (ARV) core protein sigmaA in cells of avian and mammalian origin revealed that, whereas the viral protein accumulates in the cytoplasm and nucleolus of avian cells, most sigmaA concentrates in the nucleoplasm of mammalian cells in tight association with the insoluble nuclear matrix fraction. Our results further showed that sigmaA becomes arrested in the nucleoplasm of mammalian cells via association with mammalian cell-specific factors and that this association prevents nucleolar targeting. Inhibition of RNA polymerase II activity, but not of RNA polymerase I activity, in infected mammalian cells induces nucleus-to-cytoplasm sigmaA translocation through a CRM1- and RanGTP-dependent mechanism, yet a heterokaryon assay suggests that sigmaA does not shuttle between the nucleus and cytoplasm. The scarcity of sigmaA in cytoplasmic viral factories of infected mammalian cells could account for the reported lower replicating efficiency of ARVs in mammalian versus avian cells.

Introduction

Avian reoviruses (ARVs) are icosahedral nonenveloped viruses that belong to the *Orthoreovirus* genus of the *Reoviridae* family (Mertens, 2004). They are important pathogens that cause a variety of disease conditions in birds and important losses in poultry farming (Jones, 2000; van der Heide, 2000). Avian reovirions contain a double protein capsid shell of 85 nm external diameter, which encapsulates the viral core (Zhang et al., 2005). The outer capsid is built by proteins muB, sigmaB and sigmaC, and the inner shell by proteins lambdaA, lambdaC and sigmaA. The viral core contains the RNA polymerase complex (proteins lambdaB and muA) and a segmented genome formed by 10 double-stranded RNA (dsRNA) species. Four nonstructural proteins, muNS, sigmaNS, p17 and p10, are also expressed by the ARV genome (reviewed in Benavente and Martinez-Costas, 2007).

ARV replication and morphogenesis take place exclusively within cytoplasmic phase-dense globular structures termed viral factories, which are initially formed by the nonstructural protein muNS (reviewed in Benavente and Martinez-Costas, 2006, 2007), yet two ARV proteins have been detected within the nucleus of infected cells. The nonstructural protein p17, which is encoded by the second cistron of the ARV S1 gene, accumulates in the nucleoplasm of both infected and transfected cells, but is excluded from the nucleolus. This protein shuttles continuously between the nucleus and the cytoplasm and redistributes to the cytoplasm upon inhibition of RNA polymerase II activity, suggesting that its nucleocytoplasmic distribution is transcription dependent (Costas et al., 2005). On the other hand, the S2-encoded core protein sigmaA is present the nucleolus of ARV-infected avian cells, and has been shown to enter the nucleus via a nucleoporin-dependent nondifussional mechanism that does not require added

cytosolic factors or energy input (Vazquez-Iglesias et al., 2009). These data suggest that sigmaA penetrates into the nucleus by itself using a process that is mechanistically different from the classical nuclear localization signal (NLS)/importin pathway.

ARV protein sigmaA plays a structural role by clamping together lambdaA building blocks, which is thought to stabilize core particles (Martinez-Costas et al., 2000; Yin et al., 2000; Zhang et al., 2005). Cryo-electron microscopy analysis of avian reovirions revealed that the particle contains 150 sigmaA "nodules" contacting mainly lambdaA, with minor contacts formed with the lambdaC turrets and other sigmaA molecules. The results of that study further revealed that sigmaA interacts with muB proteins of the outer shell (Zhang et al., 2005).

On the other hand, sigmaA binds dsRNA very tightly in an irreversible and sequence-independent manner (Touris-Otero et al., 2005; Yin et al., 2000). The crystal structure of a bacterially expressed recombinant sigmaA revealed that this protein binds cooperatively to dsRNA and self-assembles as helical multimers that cover the surface of the dsRNA (Guardado-Calvo et al., 2008). Finally, two reports have provided evidence that sigmaA antagonizes the interferon-induced cellular response against ARV by preventing the activation of the dsRNA-dependent protein kinase (PKR) (Gonzalez-Lopez et al., 2003; Martinez-Costas et al., 2000).

In this study we have compared the karyophilic properties of sigmaA in avian and mammalian cells. In contrast with the results obtained in avian cells, the protein accumulates in the nucleoplasm, but not the nucleolus, of mammalian cells. Nucleoplasm accumulation is due to the association of sigmaA with mammalian-specific factors, and is prevented by blocking RNA polymerase II activity, which induces sigmaA efflux into the cytoplasm by a Ran- and CRM1-dependent mechanism.

Finally, our results further revealed that, contrary to p17, sigmaA does not shuttle between the nuclear and cytoplasmic compartments of mammalian cells.

Results

SigmaA exhibits different intracellular distribution in avian and mammalian cells

To continue with the characterization of ARV core protein sigmaA, we compared its intracellular distribution in cells of avian and mammalian origin. For this, we used primary chicken embryo fibroblasts (CEF) and the stable chicken cell line DF1 as avian cells, and monkey Vero and human HeLa as representative mammalian cell lines. First of all, we analyzed the intracellular sigmaA distribution in ARV-infected cells. Immunofluorescence analysis of infected avian cells at 12 hours post-infection (h.p.i.) revealed that most sigmaA colocalized with muNS in cytoplasmic viral factories, yet a minor but significant fraction colocalized with fibrillarin in the nucleolus (Fig. 1A, rows 1-4). Strikingly, the intracellular distribution of sigmaA in infected mammalian cells was quite different (Fig. 1A, rows 5-8). First of all, most sigmaA was detected within the nucleus and only a minor fraction colocalized with muNS in cytoplasmic viral factories (Fig.1A, rows 5 and 7). Secondly, nuclear sigmaA staining accumulated in the nucleoplasm, but was excluded from nucleolus (Fig. 1A, rows 6 and 8). These data indicate that the intracellular distribution of sigmaA is different in infected avian and mammalian cells.

To determine whether the localization of sigmaA is influenced by viral factors or by changes induced by the viral infection, we next examined its distribution in transfected cells. The results shown in Fig. 1B revealed that while the viral protein accumulates in the cytoplasm and nucleolus of transfected avian cells (rows 1 and 2), it concentrates in the nucleoplasm of transfected mammalian cells (rows 3 and 4). The subnuclear sigmaA distribution was further assessed by performing import assays in digitonin-permeabilized cells (Fig. 1C). When purified bacterially expressed sigmaA was

incubated with permeabilized cells in complete transport solution (transport buffer plus energy source and cytosolic extracts), most sigmaA migrated to the nucleolus of avian cells (rows 1 and 2) and to the nucleoplasm of mammalian cells (1C, rows 3 and 4). These results demonstrate that the normal subnuclear distribution of protein sigmaA is not influenced by viral factors or by the viral infection, and further confirmed that the viral protein displays different intracellular distribution in cells of avian and mammalian origin.

SigmaA enters the nucleus of mammalian cells by a nucleoporin-dependent nondiffusional mechanism that does not require added cytosolic factors or energy input

The results of a recent report revealed that sigmaA itself is able to reach the nucleolus of avian cells, using a nucleoporin-dependent mechanism that does not require import receptors or energy input (Vazquez-Iglesias et al., 2009). The results shown in Fig. 2A revealed that sigmaA uses a similar mechanism to target the nucleoplasm of mammalian cells. Thus, our findings that sigmaA goes to the nucleus of digitonin-permeabilized Vero cells when the import assay is performed at 30 ºC (picture 1), but not when performed at 4 ºC (picture 2), indicates that sigmaA does not enter the nucleus by passive diffusion. This is reinforced by our findings that MBP-sigmaA (~90 kDa) is still able to reach the nucleus of digitonin-permeabilized Vero cells (Fig. 2C) and that GFP-sigmaA (~73 kDa) accumulates within the nucleoplasm of transfected Vero cells (not shown). On the other hand, nuclear import of sigmaA in Vero cells requires functional nucleoporins, since incubation of digitonin-permeabilized cells with wheat germ agglutinin (WGA), which binds to N-acetylglucosamine residues on nucleoporins (Yoneda et al., 1987), drastically reduces sigmaA nuclear import (picture

3). Futhermore, sigmaA was still able to reach the nucleus of digitonin-permeabilized cells when the cytosolic extract was omitted from the transport solution (picture 4), and when the cells were incubated with the inhibitors of the classical nuclear import pathway N-ethylmaleimide (NEM) and GMP-PNP (pictures 5 and 6, respectively), suggesting that sigmaA penetrates into the nucleus by an importin-independent mechanism. Finally, sigmaA was still able to target the nucleus of permeabilized Vero cells when the energy source was removed from the transport solution and when the cells were preincubated with apyrase (pictures 7 and 8, respectively), suggesting that sigmaA is imported into the nucleus by an energy-independent mechanism. It should be mentioned here that all experiments with digitonin-permeabilized cells carried out in this study were performed with both sigmaA and MBP-sigmaA as import substrates, and that identical results were obtained with the untagged and MBP-tagged protein. However, we only show the results with MBP-sigmaA in subsequent experiments because its higher molecular size (~90 kDa) avoids passive diffusion via the NPC.

We next compared the nuclear import kinetics of MBP-sigmaA with that of GST-NLS-GFP (GNG), a protein that is normally used as a control of classical nuclear import (Miyamoto et al., 2002; Yokoya et al., 1999). The intracellular accumulation of these proteins in digitonin-permeabilized Vero cells was monitored by immunofluorescence with antibodies against sigmaA and GFP, respectively. The results shown in Fig. 2B revealed that MBP-sigmaA reaches faster and more efficiently the Vero cell nucleus than GNG. Thus, whereas half of the nuclei were sigmaA-stained after 1 min of incubation, and practically 100% of the nuclei became stained 1 min later, the accumulation of GNG into the nucleus was linear over at least 20 min, and only 80% of the nuclei were stained after a 20-min incubation period. MBP-sigmaA was still able to reach the nucleus of permeabilized Vero cells when the import assay was

performed in the presence of a 20-fold excess of competitor GNG (Fig. 2C). Taken together, these results indicate that sigmaA penetrates into the nucleus using a mechanism different from the classical NLS-importin pathway.

SigmaA is anchored to the nucleoplasm of mammalian cells via association with species-specific factors

To rule out the possibility that inefficient extraction of cytosolic proteins upon digitonin permeabilization might have left behind sufficient amounts of intracellular importins as to promote sigmaA nuclear entry, digitonin-permeabilized cells were extracted with hypotonic buffer prior to assaying for transport. Hypotonic buffer extraction has been previously shown to efficiently remove soluble and nuclear pore-attached factors from permeabilized cells (Mittnacht and Weinberg, 1991; Yang et al., 1997). Both CEF and Vero cell monolayers grown on glass coverslips were permeabilized with digitonin and then incubated for 2 min on ice with hypotonic buffer containing 0.05% Triton X-100. Purified MBP-sigmaA in transport buffer lacking both cytosolic factors and energy source was subsequently added to these cells, and the intracellular localization of the viral protein was monitored by indirect immunofluorescence. Although hypotonic buffer extraction did not alter the capacity of MBP-sigmaA to translocate into the nucleolus of avian cells (Fig. 3A, compare rows 1 and 2), it changed its subnuclear target in permeabilized Vero cells. Thus, whereas MBP-sigmaA migrated to the nucleoplasm of nonextracted Vero cells (Fig. 3B, row 1), it accumulated into the nucleolus of the cells that had been extracted with hypotonic buffer (Fig. 3B, row 2). Similar results were obtained when the import assays were performed in mouse L929 and human HeLa cells (results not shown). These results

reinforced the idea that sigmaA enters the nucleus by an importin-independent pathway and further suggest that the interaction of sigmaA with hypotonic-buffer-extractable nuclear factor(s) causes its accumulation in the nucleoplasm of mammalian cells. If this is true, one would further expect that preincubation of sigmaA with extracts of mammalian cells, but not of avian cells, would restore the capacity of the viral protein to accumulate in the nucleoplasm of hypotonic-buffer-extracted permeabilized cells. Our results confirmed this hypothesis, since MBP-sigmaA redistributed to the nucleoplasm of hypotonic-buffer-extracted Vero and CEF cells when preincubated with cytosolic extracts of mammalian cells (Figs 3A and 3B, lanes 5 and 6), but not when preincubated with extracts of avian cells (Figs. 3A and 3B, lanes 3 and 4). Furthermore, MBP-sigmaA redistributed to the nucleoplasm of nonextracted CEF cells when preincubated with extracts of mammalian cells (data not shown). Taken together, these results strongly suggest that the association of sigmaA with mammalian-specific factors induces its arrest in the nucleoplasm of mammalian cells.

SigmaA associates with the nuclear matrix in an RNA-independent manner

The nuclear matrix is a nonchromatin karyoskeletal structure that remains after removal of the nuclear envelope, chromatin, and soluble factors by sequential extraction of nuclei with non-ionic detergents, DNase, and high-salt buffers (He et al., 1990). To assess whether nuclear sigmaA is bound to the nuclear matrix, ARV-infected Vero cells growing on coverslips were subjected to a series of extraction procedures that have been previously used for the preparation of the nuclear matrix fraction in situ (Tang et al., 1998). The presence of sigmaA in the different extracted fractions was monitored by indirect immunofluorescence. The results shown in Fig. 4A revealed that sigmaA

resisted extraction with cytoskeletal buffer (row 2), which is commonly used as the first extraction step in nuclear matrix preparations to remove tightly bound nuclear proteins (Yang et al., 1997). It also resisted further extraction with 0.25 M ammonium sulphate after DNase digestion (row 3), which extracts the DNA and the majority of the DNA-binding proteins, as evidenced by the release of histone H1 (row 3). The fact that a significant sigmaA fraction remained confined within nuclei after subsequent solubilization by 2 M NaCl (row 4), suggests that the viral protein is tightly associated with the insoluble fraction of the nuclear matrix, and not to chromatin.

Since sigmaA is an RNA binding protein and since the nuclear matrix contains both proteins and RNAs, sigmaA might be associated to the matrix in an RNA-dependent manner. To test this possibility, ARV-infected Vero cells were fixed with methanol, then incubated with DNase I or RNase A, and finally subjected to immunofluorescence microscopy analysis after staining with antibodies against sigmaA and nucleophosmine/B23. B23 was used as a positive control because it is a nucleolar RNA-binding protein that is removed from the nucleus upon RNase treatment (Hirano et al., 2009). In untreated fixed cells, sigmaA was concentrated in the nucleoplasm whereas most B23 was localized within the nucleolus (Fig. 4B, row 1). The normal subnuclear distribution of the two proteins was not altered by treating the cells with DNase, suggesting that they are not DNA binding proteins (Fig. 4B, row 2). As expected, the nucleolar fluorescence signal of B23 disappeared from the nucleolus upon treating the fixed cells with RNase A (Fig. 4B, row 3, middle picture). In contrast, the normal nucleoplasmic accumulation of sigmaA was not perturbed by the RNase treatment (Fig. 4B, row 3, left picture). Taken together, these results suggest that sigmaA associates with the nuclear matrix of mammalian cells in an RNA-independent manner.

Inhibition of RNA polymerase II activity induces sigmaA redistribution to the cytoplasm

The nucleocytoplasmic distribution of a number of proteins is influenced by the transcriptional activity of the cell. Some nuclear proteins migrate to the cytoplasm upon inhibition of transcription (Pinol-Rama and Dreyfuss, 1991), whereas others require ongoing RNA polymerase activity for nuclear export (Khacho et al., 2008). To investigate the transcription dependence of nuclear sigmaA accumulation in mammalian cells, the effect of RNA polymerase inhibitors was investigated. For this, ARV-infected Vero cells were treated for 5 h with cycloheximide (20 μg/ml) plus concentrations of actinomycin D (AMD) that inhibit the activity of RNA polymerase I (0.05 μg/ml) and RNA polymerase II (0.5 μg/ml). We first checked the effectiveness of our AMD in Vero cells by showing that incubation of these cells with 0.05 μg/ml of AMD induces nucleolus-to-nucleoplasm redistribution of nucleophosmine/B23 (Fig. 5A), a situation similar to that previously reported for mouse embryonic fibroblasts (Meder et al., 2004). In contrast, sigmaA remained confined within the nucleoplasm of Vero cells treated with 0.05 μg/ml of AMD (Figs. 5A and 5B, row 2), suggesting that nuclear sigmaA accumulation is not dependent on RNA polymerase I activity. However, nucleus-to-cytoplasm redistribution of sigmaA took place when infected Vero cells were incubated in the presence of 0.5 μg of AMD/ml (Fig. 5B, row 3) or the RNA polymerase II inhibitors α-amanitin and DRB (Fig. 5B, rows 4 and 5, respectively). The shift in sigmaA distribution did not however occur when the cells were incubated with cycloheximide alone (Fig. 5B, row 1), indicating that the cytoplasmic accumulation of this protein is likely the result of transcription inhibition rather than inhibition of protein synthesis.

DRB-induced cytoplasmic accumulation of sigmaA was reversed when Vero cells were subsequently incubated in DRB-free medium (Fig. 5B, row 6), suggesting that ongoing transcription is required for sigmaA nuclear import. To test this hypothesis we performed import assays in Vero cells that had been preincubated for 3 h with different AMD concentrations before digitonin permeabilization. The results shown in Fig. 5C revealed that while MBP-sigmaA still reaches the nucleus of permeabilized cells that had been preincubated with 0.05 μg of AMD/ml (row 2, left picture), the protein does not enter the nucleus of the cells that had been preincubated with 0.5 μg of AMD/ml (row 3, left picture). However, the latter treatment did not prevent GNG from reaching the nucleus of digitonin-permeabilized Vero cells (Fig. 5C, left picture of row 3), supporting the notion that transcription inhibitors do not inhibit nuclear import mediated by classical NLSs (Pinol-Roma and Dreyfuss, 1991; Stauber et al., 2001). These results indicate that sigmaA nuclear export and import are coupled to RNA polymerase II activity.

Inhibition of RNA polymerase II activity promotes sigmaA nuclear export via a Ran- and CRM1-dependent pathway

We next investigated the mechanism by which sigmaA exits the nucleus after RNA polymerase II inhibition. As shown in Fig. 6A, sigmaA redistributes to the cytoplasm when ARV-infected Vero cells were incubated in the presence of 0.5 μg/ml of AMD at 37 ºC (row 2), but not when the incubation was performed at 4 ºC (row 3), indicating that sigmaA nuclear export is a temperature-dependent process.

It has been reported that cellular ATP depletion induces a major drop in both free GTP and the nuclear concentration of Ran-GTP, which in turn leads to inhibition of

classical nuclear transport, because a nuclear Ran-GTP pool is required for both the assembly of export complexes and the disassembly of import complexes (Schwoebel et al., 2002). To determine whether sigmaA nuclear export observed upon RNA polymerase II arrest is a Ran-dependent process, we compared the effect of AMD on sigmaA localization in ATP-depleted and -nondepleted infected Vero cells. Incubation of ARV-infected Vero cells for 15 min in the presence of 10 mM sodium azide and 10 mM deoxyglucose caused a drop in the intracellular ATP level to 4% of its normal value (determined with the FLASC Sigma-Aldrich kit), and abolished the capacity of AMD to induce nucleus-to-cytoplasm sigmaA redistribution (Fig. 6A, compare rows 2 and 4). These results suggest that, contrary to nuclear import, sigmaA nuclear export is an energy- and Ran-dependent process.

Chromosome region maintenance 1 (CRM1) is a member of the importin-β family and a nuclear export receptor for many different classes of cellular proteins and for specific RNAs, which is specifically and potently inhibited by the antifungal cytotoxin leptomycin B (LMB) (Kudo et al., 1999). Within the nucleus, CRM1 associates with both Ran-GTP and cargo proteins that possess a leucine-rich nuclear export signal (NES), and the trimeric complex crosses the nuclear pore to deliver the cargo protein in the cytoplasm (Fornerod et al., 1997). To determine whether the cytoplasmic accumulation of sigmaA observed after RNA polymerase II inhibition reflects nuclear export through a CRM1-dependent pathway, we investigated the effect of LMB, both alone and in the presence of AMD, on the intracellular localization of ARV proteins sigmaA and p17 in ARV-infected Vero cells. We used p17 as a control protein because we have previously shown that AMD induces its nuclear exclusion via a CRM1-independent pathway (Costas et al., 2005). Infected Vero cells were incubated for 5 h in culture medium supplemented with 20 μg of cycloheximide/ml plus either: i) 30 ng of

LMB/ml; ii) 0.5 μg of AMD/ml; or iii) 0.5 μg of AMD/ml plus 30 ng of LMB/ml. Most sigmaA and p17 remained associated to the nucleoplasm when infected cells were incubated with LMB alone (Fig. 6B, row 1), indicating that the antifungal cytotoxin does not alter the normal nuclear distribution of these proteins. However, LMB was able to block the capacity of AMD to induce nucleus-to-cytoplasm translocation of sigmaA (Fig. 6B, compare rows 2 and 3, right pictures), but not of p17 (Fig. 6B, compare rows 2 and 3, middle pictures). A similar LMB effect was obtained in sigmaA-transfected cells (result not shown). These data demonstrate that sigmaA, but not p17, uses a CRM1-dependent pathway to exit the nucleus upon RNA polymerase II inhibition.

SigmaA does not shuttle between the nuclear and cytoplasmic compartments

Many nuclear proteins are permanently trapped within the nucleus, whereas others have the ability to shuttle between the nucleus and cytoplasm (reviewed in Nigg, 1997). Since many nuclear proteins whose nuclear accumulation is coupled to RNA polymerase activity are able to recirculate between the nucleus and the cytoplasm, we examined the nucleocytoplasmic shuttling properties of ARV protein sigmaA. To accomplish this, we performed an in vivo interspecies heterokaryon assay that has been used to characterize the shuttling properties of nuclear proteins (Fan and Steitz, 1998; Inman et al., 2002; Michael et al., 1997), and that we have successfully used to document the shuttling activity of the ARV nonstructural p17 protein (Costas et al., 2005). Monkey Vero cells were co-transfected with the recombinant plasmids pEGFP-p17 and pCDNA3.1-sigmaA and 24 h later the cells were fused with untransfected mouse L929 cells in the presence of 50% polyethylene glycol. The fused cells were then incubated for different times in the presence of 100 μg of cycloheximide/ml and

processed for immunofluorescence analysis. Monkey and mouse nuclei in heterokaryons can be distinguished by Hoechst staining, since monkey nuclei display a relatively diffuse stain, whereas the nuclei of rodent cells exhibit a characteristic punctuate pattern due to intranuclear body staining (Fan and Steitz, 1998). The presence of sigmaA in mouse nuclei of heterokaryons would indicate that the protein was able to exit the monkey nuclei and to penetrate into the nuclei of untransfected mouse cells. The results shown in Fig. 7 revealed that GFP-associated fluorescence was localized in both monkey and mouse nuclei of heterokaryons at both 4 and 15 h after cell fusion (middle pictures), confirming our previous observation that p17 is a nucleocytoplasmic shuttling protein (Costas et al., 2005). In clear contrast, sigmaA staining remained confined exclusively within the Vero cell nuclei at the two times tested (right pictures), indicating that sigmaA is unable to translocate from donor-transfected nuclei into recipient mouse nuclei, and hence that it does not traffic between the nucleus and cytoplasm of Vero cells.

Discussion

In this study we have examined the karyophilic properties of ARV protein sigmaA in mammalian cells. Our data showed that, as in avian cells, sigmaA is able to enter the nucleus of mammalian cells by a nondiffusional energy- and importin-independent mechanism and that its presence within the nucleus is not promoted by viral factors or by changes induced by the viral infection. This is supported by our findings that sigmaA enters the nucleus of digitonin-permeabilized cells faster and more efficiently than an NLS-containing protein, and that sigmaA is still able to reach the nucleus of permeabilized Vero cells when the import assay was performed in the presence of a 20-fold excess of competitor GNG.

One striking and interesting finding of this study is that sigmaA was detected in the nucleolus of avian cells and in the nucleoplasm of mammalian cells, suggesting that its nuclear distribution is controlled by species-specific factors or by alternative posttranslational modifications. Our finding that bacterially-expressed MBP-sigmaA is imported into the nucleolus of avian cells and into the nucleoplasm of mammalian cells suggests that posttranslational modifications do not likely play a role in sigmaA localization. Extraction of digitonin-permeabilized cells with hypotonic buffer revealed that sigmaA becomes arrested in the nucleoplasm of mammalian cells by binding to mammalian-specific factors, which in turn suggests that the nucleolus is the normal sigmaA target, and that the viral protein is unable to reach the nucleolus of mammalian cells because it is anchored to the nucleoplasm via association with mammalian-specific factors. In order to characterize these factors, we are currently trying to identify sigmaA-interacting proteins that are present in extracts of Vero cells, but not in those of avian cells, as well as sigmaA-interacting proteins that are eluted from digitonin-permeabilized Vero cells upon extraction with hypotonic buffer.

Distinct subnuclear localization is not the only difference observed in the intracellular distribution of sigmaA in avian versus mammalian cells. Our data further showed that, whereas most sigmaA is present in the cytoplasm of infected avian cells, only a minor fraction of the viral protein is detected in the cytoplasm of infected mammalian cells. Since sigmaA is a structural core protein whose presence in cytoplasmic viral factories is required to form progeny viral particles, the scarcity of sigmaA in cytoplasmic inclusions of infected mammalian cells could account for the reported observation that ARVs replicate with much lower efficiency in mammalian cells than in avian cells (Mallo et al., 1991a, b).

The inhibition of RNA polymerase II activity in ARV-infected mammalian cells

induces sigmaA redistribution to the cytoplasm, and the effect of LMB on the AMD-induced nuclear export indicates that sigmaA exits the mammalian cell nucleus via a canonical CRM1-dependent pathway. This in turn suggest that sigmaA nuclear export requires RanGTP, since all CRM1-mediated export requires RanGTP (Fornerod et al., 1997; Fukuda et al., 1997), and since cellular ATP depletion, which drastically reduces the nuclear pool of RanGTP (Schwoebel et al., 2002), also impairs sigmaA nuclear exit. We do not know yet whether sigmaA exits the nucleus of mammalian cells after AMD treatment by binding directly to CRM1/RanGTP or whether it uses the nuclear export signal (NES) of a sigmaA-associated protein to cross the nuclear pore in a piggy-back fashion. In contrast, inhibition of both RNA polymerase I and II activities did not avoid nucleolar sigmaA accumulation in infected avian cells (not shown), suggesting that the effect of RNA polymerase II inhibitors on sigmaA nuclear exit in mammalian cells is an indirect effect on sigmaA-associated proteins. This is supported by our findings that sigmaA does not recirculate between the nucleus and the cytoplasm of transcription-competent mammalian cells and that sigmaA is retained in the nucleoplasm of mammalian cells by association with mammalian-specific factors. Inhibition of transcription, which induces the reorganization of many subnuclear compartments and the proteins that form them (Dundr and Misteli, 2001), could release the masked CRM1-dependent NES of a sigmaA-associated protein, thus allowing sigmaA to exit the nucleus in a piggy-back fashion, as has been reported for other proteins (Foo et al., 2007; Hamilton et al., 1997; Li et al., 2008).

To our knowledge only one other viral protein has been previously reported to display different localization in mammalian versus avian cells. Protein 3b of infectious bronchitis virus (IBV), a virus that normally infects chickens, has been shown to localize to the nucleus when transiently-expressed in vaccinia virus-infected

mammalian cells, but to the cytoplasm of both IBV-infected and transfected avian cells (Pendleton et al., 2006). The results of this study and the ones presented in this manuscript highlight the importance of using cells derived from the natural host when analyzing molecular aspects of viral replication and when studying the properties of viral proteins. Accordingly, the conclusions reached by studying the replication of ARVs in mammalian cells should be taken with caution, unless the results are reproduced in avian cells.

Materials and methods

Cells, viruses, antibodies, plasmids and reagents

Primary cultures of CEF were prepared from 9- to 10-day old chicken embryos and grown in medium 199 supplemented with 10% tryptose phosphate broth and 5% calf serum. Strain 1733 of ARV was grown on semiconfluent monolayers of primary CEF as previously described (Grande and Benavente, 2000). Chicken DF1, monkey Vero, mouse L929 and human HeLa cells were grown in monolayers in medium DMEM supplemented with 10 % fetal bovine serum.

The generation of monoclonal and polyclonal antibodies against sigmaA and muNS has been described (Martinez-Costas et al., 2000; Touris-Otero et al., 2004). Anti-fibrillarin (mouse monoclonal, clone AFBN01) was purchased from Cytoskeleton, Inc. (Denver, Col.). Anti-B23 (mouse monoclonal, clone FC-8791) and anti-histone H1 (mouse monoclonal, clone AE-4) were from Santa Cruz Biotechnology Inc. (Heidelberg, Germany), and anti-GFP was from Roche (Barcelona, Spain). Alexa Fluor 594 goat anti-mouse (red; #A11005) Alexa Fluor 594 goat anti-rabbit (red; #A11012), Alexa Fluor 488 goat anti-mouse (green; #A11001), and Alexa-Fluor 488 goat anti-rabbit (green; #A11008) fluorescent-conjugated secondary antibodies were purchased from Invitrogen (Barcelona, Spain).

The generation of plasmids pMal-sigmaA (for bacterial expression of MBP-sigmaA), pEGFP-sigmaA (for eukaryotic expression of GFP-sigmaA), pCDNA3.1-sigmaA (for eukaryotic expression of full-length sigmaA), pEGFP-p17 (for eukaryotic expression of GFP-p17) has been previously described (Costas et al., 2005; Vazquez-Iglesias et al., 2009). The plasmid for bacterial expression of GST-NLS-GFP (GNG) has been reported

(Miyamoto et al., 2002; Yokoya et al., 1999). Digitonin, WGA and Mowiol were purchased from Calbiochem (Darmstadt, Germany). All other reagents used in this study were from Sigma-Aldrich.

Infections, transfections, heterokaryon formation and fluorescence microscopy

Infection of avian and mammalian cells by ARV has been described (Grande and Benavente, 2000). Transfections of cell monolayers were done with Lipofectamine (Invitrogen), according to the manufacturer's instructions. Transfected cells were incubated at 37 °C for 24 h, unless otherwise stated. For ATP depletion, cell monolayers were incubated for 15 min in PBS containing 10% fetal bovine serum, 10 mM sodium azide and 10 mM 2-deoxyglucose (Schwoebel et al., 2002). ATP-depleted cells were subsequently incubated for the indicated times in the same medium supplemented with 5 μg of actinomycin D (AMD)/ml.

For heterokaryon assays, Vero cell monolayers were co-transfected with plasmids expressing GFP-p17 and sigmaA, and 24 h later the cells were detached by trypsinization, placed on coverslips and incubated for 15 h at 37 ºC. Heterokaryons were generated by fusing transfected Vero cells with untransfected mouse L929 cells in the presence of 50% polyethylene glycol. The fused cells were incubated for different times in the presence of 100 μg of cycloheximide/ml as previously described (Costas et al., 2005; Fan and Steitz, 1998).

For indirect immunofluorescence microscopy, cell monolayers were grown on coverslips and infected or transfected. At the indicated times, monolayers were washed twice with PBS and fixed either for 10 min at room temperature in 4% paraformaldehyde in PBS, or for 15 min at -20 ºC in 100% methanol.

Paraformaldehyde-fixed cells were washed twice with PBS, incubated for 3 min in permeabilizing buffer (0.5% Triton X-100 in PBS) and then blocked in PBS containing 2% bovine serum albumin for 30 min at room temperature. Methanol-fixed cells were washed twice with PBS and blocked for 30 min at room temperature in PBS containing 2% bovine serum albumin. All fixed cells were incubated for 1 h at room temperature with primary antibodies diluted in blocking buffer. After three washes with PBS, the cells were incubated for 30 min with secondary antibodies and DAPI. Cell-containing coverslips were then washed six times with PBS and mounted on glass slides. Images were obtained with an Olympus DP-71 digital camera mounted on an Olympus BX51 fluorescence microscope. Images were processed with Adobe Photoshop (Adobe Systems, California, USA).

Bacterial expression and purification of recombinant proteins, and import assays

The expression and purification of MBP-sigmaA, sigmaA and GNG have been described (Guardado-Calvo et al., 2008; Hermo-Parrado et al., 2007; Miyamoto et al., 2002; Yokoya et al., 1999). Preparation of cytosolic extracts, digitonin permeabilization and import assays all were performed as described previously (Vazquez-Iglesias et al., 2009).

Nuclease treatment and nuclear matrix preparation

For nuclease treatment, monolayers of ARV-infected Vero cells growing on coverslips were fixed for 2 min in methanol at -20 ºC, rinsed with PBS and incubated with either RNase A (100 ug/ml in PBS) or DNase I (40 U/ml in PBS supplemented

with 5 mM $MgCl_2$) for 2 h at room temperature (Hirano et al., 2009). Cells were then washed several times with PBS and processed for immunofluorescence.

Nuclear matrix preparation was performed essentially as previously described (Tang et al., 1998). Infected Vero cells growing on coverslips were washed with cold PBS and extracted with CSK buffer (10 mM PIPES-NaOH pH 6.8, 100 mM NaCl, 300 mM sucrose, 3 mM $MgCl_2$, 1 mM EGTA, and 0.5% Triton X-100) for 5 minutes at 4ºC. The buffer was then removed and the cells were incubated in DNase buffer (10 mM PIPES-NaOH pH 6.8, 50 mM NaCl, 300 mM sucrose, 3 mM $MgCl_2$, 0.5% Triton X-100, and 40 U of RNase-free DNase I/ml) for 1 h at 37 ºC. Nuclease-treated cells were sequentially extracted with 0.25 M ammonium sulphate in CSK buffer for 5 min at room temperature, and then with 2 M NaCl in CSK buffer. Cell monolayers were fixed after each extraction step and processed for immunofluorescence.

Acknowledgements

We thank Laboratorios Intervet (Salamanca, Spain) for providing pathogen-free embryonated eggs, and Drs. William Hall and Yoshihiro Yoneda for their generosity in providing plasmids and antibodies used in this study. We are also grateful to Rebeca Menaya and Leticia Barcia for their excellent technical assistance and to Mark van Raaij for critical reading of the manuscript. This research was supported by grants from the Spanish Ministerio de Ciencia y Tecnología (BFU2007-61330/BMC) and from the Xunta de Galicia (08CSA009203PR). L. V-I. and I. L-S. were recipients of predoctoral fellowships from the FPI and FPU programs of the Spanish Ministerio de Ciencia y Tecnología.

References

Benavente, J., Martinez-Costas, J., 2006. Early steps in avian reovirus morphogenesis. Curr. Top. Microbiol. Immunol. 309, 67-85.

Benavente, J., Martinez-Costas, J., 2007. Avian reovirus: structure and biology. Virus Res. 123, 105-119.

Costas, C., Martinez-Costas, J., Bodelon, G., Benavente. J., 2005. The second open reading frame of the avian reovirus S1 gene encodes a transcription-dependent and CRM1-independent nucleocytoplasmic shuttling protein. J. Virol. 79, 2141-2150.

Dundr, M., Misteli, T., 2001. Functional architecture in the cell nucleus. Biochem. J. 356, 297-310.

Fan, X.C., Steitz, J.A., 1998. HNS, a nuclear-cytoplasmic shuttling sequence in HuR. Proc. Natl. Acad. Sci. U. S. A. 95, 15293-15298.

Foo, R.S., Nam, Y.J., Ostreicher, M.J., Metzl, M.D., Whelan, R.S., Peng, C.F., Ashton, A.W., Fu, W., Mani, K., Chin, S.F., Provenzano, E., Ellis, I., Figg, N., Pinder, S., Bennet, M.R., Caldas, C., Kitsis, R.N., 2007. Regulation of p53 tetratimerization and nuclear export by ARC. Proc. Natl. Acad. Sci. U. S. A. 104, 20826-20831.

Fornerod, M., Ohno, M., Yoshida, M., W. Mattaj, I., 1997. CRM1 is an export receptor for leucine-rich nuclear export signals. Cell 90, 1051-1060.

Fukuda, M., Asano, S., Nakamura, T., Adachi, M., Yoshida, M., Yanagida, M., Nishida, E., 1997. CRM1 is responsible for intracellular transport mediated by the nuclear export signal. Nature 390, 308-311.

Gonzalez-Lopez, C., Martinez-Costas, J., Esteban, M., Benavente, J., 2003. Evidence that avian reovirus σA protein is an inhibitor of the double-stranded RNA-dependent

protein kinase. J. Gen. Virol. 84, 1629-1639.

Grande, A., Benavente, J., 2000. Optimal conditions for the growth, purification and storage of avian reovirus S1133. J. Virol. Methods 85, 43-54.

Guardado-Calvo, P., Vazquez-Iglesias, L., Martinez-Costas, J., Llamas-Sainz, A.L., Schoehn, G., Fox, G.C., Hermo-Parrado, L., Benavente, J., van Raaij, M.J., 2008. Crystal structure of the avian reovirus inner capsid protein σA. J. Virol. 82, 11208-11216.

Hamilton, B.J., Burns, C.M., Nichols, R.C., Rigby, W.F., 1997. Modulation of AUUUUA response element binding by heterogeneous nuclear ribonucleoprotein A1 in human T lymphocytes. The roles of cytoplasmic location, transcription, and phosphorylation. J. Biol. Chem. 272, 28732-28741.

He, D., Nickerson, J.A., Penman, S., 1990. Core filaments of the nuclear matrix. J. Cell Biol. 110, 569-580.

Hermo-Parrado, X.L., Guardado-Calvo, P., Llamas-Saiz, A.L., Costas, C., Martinez-Costas, J., Benavente, J., van Raaij, M.J., 2007. Crystallization of the avian reovirus double-stranded RNA-binding and core protein sigmaA. Acta Crystallogr. F 63, 426-429.

Hirano, Y., Ishii, K., Kumeta, M., Furukawa, K., Takeyasu, K., Horigome, T., 2009. Proteomic and targeted analytical identification of BXDC1 and EBNA1BP2 as dynamic scaffold proteins in the nucleolus. Genes Cells 14, 155-166.

Inman, G.J., Nicolas, F.J., Hill, C.S., 2002. Nucleocytoplasmic shuttling of Smad2, 3, and 4 permits sensing of TGF-beta receptor activity. Mol. Cell 10, 283-294.

Jones, R. C., 2000. Avian reovirus infections. Rev. Sci. Tech. 19, 614-625.

Khacho, M., Mekhail, K., Pilon-Larose, K., Payette, J., Lee, S., 2008. Cancer-causing mutations in a novel transcription-dependent nuclear export motif of VHL abrogate

oxygen-dependent degradation of hypoxia-inducible factor. Mol. Cell Biol. 28, 302-314.

Kudo, N., Matsumori, N., Taoka, H., Fujiwara, D., Schreiner, E.P., Wolff, B., Yoshida, M., Horinouchi, S., 1999. Leptomycin B inactivates CRM1/exportin 1 by covalent modification at a cysteine residue in the central conserved region. Proc. Natl. Acad. Sci. U. S. A. 96, 9112-9117.

Li, W., Yu, S., Liu, T., Kim, J.H., Blank, V., Li, H., Kong, A.N., 2008. Heterodimerization with small Maf proteins enhances nuclear retention of Nrf2 via masking the NESzip motif. Biochim. Biophys. Acta 1783, 1847-1856.

Mallo, M., Martinez-Costas, J., Benavente, J., 1991a. Avian reovirus S1133 can replicate in mouse L cells: effect of pH and cell attachment status on viral infection. J. Virol. 65, 5499-5505.

Mallo, M., Martinez-Costas, J., Benavente, J., 1991b. The stimulatory effect of actinomycin D on avian reovirus replication in L cells suggests that translational competition dictates the fate of the infection. J. Virol. 65, 5506-5512.

Martinez-Costas, J., Gonzalez-Lopez, C., Vakharia, V.N., Benavente, J., 2000. Possible involvement of the double-stranded RNA-binding core protein sigmaA in the resistance of avian reovirus to interferon. J. Virol. 74, 1124-1131.

Meder, V.S., Boeglin, M., de Murcia, G., Schreiber, V., 2004. PARP-1 and PARP-2 interact with nucleophosmin/B23 and accumulate in transcriptionally active nucleoli. J. Cell Sci. 118, 211-222.

Mertens, P., 2004. The dsRNA viruses. Virus Res. 101, 3-13.

Michael, W.M., Eder, P.S., Dreyfuss, G., 1997. The K nuclear shuttling domain: a novel signal for nuclear import and nuclear export in the hnRNP K protein. EMBO J. 16, 3587-3598.

Mittnacht, S., Weinberg, R.A., 1991. G1/S phosphorylation of the retinoblastoma protein is associated with altered affinity for the nuclear compartment. Cell 65, 381-393.

Miyamoto, Y., Hieda, M., Harreman, M.T., Fukumoto, M., Saiwaki, T., Hotel, A.E., Corbett, A.N., Yoneda, Y., 2002. Importin α can migrate into the nucleus in an importin β- and Ran-independent manner. EMBO J. 21, 5833-5842.

Nigg, E.A., 1997. Nucleocytoplasmic transport: signals, mechanisms and regulation. Nature 386, 779-787.

Pendleton, A.R., Machamer, C.E., 2006. Different localization and turnover of infectious bronchitis virus 3b protein in mammalian versus avian cells. Virology 345, 337-345.

Pinol-Roma, S., Dreyfuss, G., 1991. Transcription-dependent and transcription-independent nuclear transport of hnRNP proteins. Science 253, 312-314.

Schwoebel, E.D., Ho, T.H., Moore, M.S., 2002. The mechanism of inhibition of Ran-dependent nuclear transport by cellular ATP depletion. J. Cell Biol. 157, 963-974.

Stauber, R.H., Krätzer, F., Schneider, G., Hirschmann, N., Hauber, J., 2001. Investigation of nucleocytoplasmic transport using UV-guided microinjection. J. Cell. Biochem. 80, 388-396.

Tang, Y., Getzenberg, R.H., Vietmeier, B.N., Stallcup, M.R., Eggert, M., Renkawitz, R., DeFranco, D.B., 1998. The DNA-binding and τ2 transactivation domains of the rat glucocorticoid receptor constitute a nuclear matrix-targeting signal. Mol. Endocrinol. 12, 1420-1431.

Tourís-Otero, F., Martínez-Costas, J., Vakharia, V.N., Benavente, J., 2004. Avian reovirus nonstructural protein μNS forms viroplasm-like inclusions and recruits σNS to these structures. Virology 319, 94-106.

Tourís-Otero, F., Martínez-Costas, J., Vakharia, V.N., Benavente, J., 2005. Characterization of the nucleic acid-binding activity of the avian reovirus non-structural protein σNS. J. Gen. Virol. 86, 1159-1169.

van der Heide, L., 2000. The history of avian reovirus. Avian Dis. 44, 638-641.

Vazquez-Iglesias, L., Lostale-Seijo, I., Martinez-Costas, J., Benavente, J., 2009. Avian reovirus sigmaA localizes to the nucleolus and enters the nucleus by a nonclassical energy- and carrier-independent pathway. J. Virol. 83, 10163-10175.

Yang, J., Liu, J., DeFranco, D.B., 1997. Subnuclear trafficking of glucocorticoid receptors in vitro: chromatin recycling and nuclear export. J. Cell Biol. **137,** 523-538.

Yin, H.S., Shien, J.H., Lee, L.H., 2000. Synthesis in Escherichia coli of avian reovirus core protein σA and its dsRNA-binding activity. Virology 266, 33-41.

Yokoya, F., Imamoto, M., Tachibana, T., Yoneda, Y., 1999. β-catenin can be transported into the nucleus in a Ran-unassisted manner. Mol. Biol. Cell 10, 1119-1131.

Yoneda, Y., Imamoto-Sonobe, N., Yamaizumi, M., Uchida, T., 1987. Reversible inhibition of protein import into the nucleus by wheat germ agglutinin injected into cultured cells. Exp. Cell Res. 173, 586–595.

Zhang, X., Tang, J., Walker, S.B., O'Hara, D., Nibert, M.L., Duncan, R., Baker, T.S., 2005. Structure of avian orthoreovirus virion by electron cryomicroscopy and image reconstruction. Virology 343, 25-35.

Figure legends

Fig. 1. Intracellular sigmaA distribution in avian and mammalian cells. (A) Semiconfluent monolayers of the avian and mammalian cells indicated on the left were infected with 10 and 50 PFU/cell, respectively, of ARV 1733 for 12 h. The cells were then fixed and immunostained green for sigmaA (left pictures) and red for muNS or fibrillarin and blue with DAPI (right pictures). Stained cells were visualized with a fluorescence microscope. (B) Semiconfluent monolayers of the cells indicated on the left were transfected with the pCDNA3.1-sigmaA plasmid and 24 h later the cells were processed for immunofluorescence analysis. The cells in the left lane were stained green for sigmaA, and in the right lane were further stained red for fibrillarin and blue with DAPI. White arrows point to the nucleoli of avian cells. Nuclear envelopes of sigmaA-containing cells in the left pictures of panels A and B are labeled with dots. (C) Monolayers of the cells indicated on the left were grown on coverslips and permeabilized with digitonin. The cells were subsequently incubated for 30 min at 30 ºC with purified sigmaA dissolved in complete transport solution and processed for immunofluorescence analysis. The cells in the left pictures were stained green for sigmaA and in the right pictures were further stained red for fibrillarin and counterstained blue with DAPI. Black scale bars: 20 μm.

Fig. 2. Characteristics of sigmaA nuclear import in Vero cells. (A) Vero cell monolayers were permeabilized with digitonin and then incubated with purified sigmaA (0.2 mg/ml) at 30 ºC (pictures 1 and 3-8) or 4 ºC (picture 2) in 50 μl of complete transport solution (pictures 1-3) or of transport solution lacking cytosolic extract (pictures 4-6) or cytosolic extract and energy source (pictures 7 and 8). The cells in

pictures 3, 5, 6 and 8 were preincubated at room temperature with transport buffer containing 500 μg of WGA/ml (picture 3), 5 mM NEM (picture 5), 1 mM GMP-PNP (picture 6) or 25 U apyrase/ml (picture 8), as described in detail elsewhere (Vazquez-Iglesias et al., 2009). The cells were immunostained green for sigmaA. (B) Permeabilized Vero cell monolayers were incubated with the import substrates MBP-sigmaA or GNG in complete transport solution for the times indicated, then fixed and immunostained for GNG and sigmaA. The percentage of stained nuclei was plotted against the incubation time. For each experiment 100 cells were counted, and each time point is the mean of three independent experiments. Error bars indicate standard deviation of the mean. (C) Permeabilized Vero cells were incubated with 50 μl of complete transport solution containing 0.2 mg/ml MBP-sigmaA (row 1) or 0.2 mg/ml MBP-sigmaA plus 4 mg/ml GNG. After 30 min at 30°C, the cells were fixed, stained red for MBP-sigmaA and counterstained blue with DAPI. The cells were visualized by fluorescence microscopy, and GNG is stained in green. Black scale bars: 20 μm.

Fig. 3. Effects of hypotonic buffer extraction and cytosolic extract supplementation on sigmaA nuclear targeting. Import assays in CEF (A) and Vero (B) cells were performed using MBP-sigmaA dissolved in transport solution lacking energy source and cytosolic extract (row 1). Import assays in rows 2-6 were performed with hypotonic-buffer-extracted cells, after preincubating the MBP-sigmaA import substrate with buffer (row 2) or with cytosolic extracts from the cells indicated on the right (rows 3-6). The cells were then fixed, stained blue with DAPI and immunostained green for sigmaA and red for fibrillarin. Black scale bars: 20 μm.

Fig. 4. Buffer extraction and nuclease digestion. (A) ARV-infected Vero cells were extracted (rows 2-4) or not (row 1) with cytoskeletal buffer. The cells in rows 3 and 4 were subjected to DNase I digestion (40 U/ml, 1h at 37 ºC) and then extracted with 0.25 ammonium sulphate (row 3). The cells in row 4 were further extracted with 2 M NaCl. The cells were stained blue with DAPI (right pictures), and immunostained green for sigmaA (left pictures) and red for histone H1 (middle pictures). (B) ARV-infected Vero cells were fixed for 2 min in methanol at -20 ºC (row 1), then incubated for 2 h at room temperature with PBS (row 1), 40 U of DNase I/ml (row 2) or 100 μg of RNase A/ml (row 3). The cells were then fixed, stained blue with DAPI (right pictures), and immunostained green for sigma (left pictures) and red for B23 (middle pictures). Black scale bars: 20 μm.

Fig. 5. Effect of transcription inhibitors on nuclear accumulation. (A) At 14 h.p.i. infected Vero cells were incubated for 5 h at 37 ºC with 20 μg of cycloheximide/ml (row 1) or with cycloheximide plus 0.05 μg of AMD/ml (row 2), and then processed for immunofluorescence. The cells were stained blue with DAPI (righ pictures) and immunostained green for sigmaA (left pictures) and red for nucleophosmine/B23 (middle pictures). (B) At 9 h.p.i. ARV infected Vero cells were incubated for 5 h at 37 ºC with 20 μg of cycloheximide/ml (row 1) plus the concentrations of the inhibitors indicated on the left of rows 2-6. The cells in row 6 were subsequently incubated for another 5 h in DRB-free medium. The cells in the left pictures were stained green for sigmaA, and in the right pictures were further stained red for fibrillarin and conterstained blue with DAPI. (C) Vero cells were incubated for 3 h with the concentrations of the inhibitors indicated on the left, then permeabilized with digitonin and incubated with MBP-sigmaA dissolved in transport buffer (left lane) or GNG

dissolved in complete transport buffer (right lane). The cells were immunostained green for sigmaA (left pictures) and visualized by fluorescence microscopy. Black scale bars: 20 μm.

Fig. 6. Effect of inhibitors on sigmaA nuclear exit. (A) ARV-infected Vero cells were incubated for 5 h with cycloheximide (row 1) or with cycloheximide plus 0.5 μg of AMD/ml, at either 37 ºC (rows 2 and 4) or 4ºC (row 3). In row 4 the cells were ATP depleted by incubation with sodium azide and deoxyglucose, starting 15 min before the AMD treatment and during the treatment. The cells were then fixed, immunostained green for sigmaA (left pictures) and blue with DAPI (right pictures). (B) ARV-infected Vero cells were incubated for 5 h at 37 ºC with cycloheximide plus the inhibitors shown at the left. The cells were subsequently fixed, stained blue with DAPI (left pictures) and immunostained green for p17 (middle pictures) and red for sigmaA (right pictures). Black scale bars: 20 μm.

Fig. 7. Heterokaryon assay. Semiconfluent Vero cell monolayers were co-transfected with pCDNA3.1-sigmaA and pEGFP-p17 plasmids, and 24 h later the cells were scrapped off the plate. Aliquots of 5 x 10^5 transfected cells were then fused with the same amount of untransfected mouse L929 cells in the presence of 50% polyethylene glycol 4000 plus 100 μg of cycloheximide/ml. At the post-fusion times indicated at the right, the cells were fixed, stained blue with DAPI (left pictures) and immunostained red for sigmaA (right pictures). GFP-p17 is stained green (middle pictures). Cells of two representative experiments are shown for each time point. White arrows in left pictures point towards acceptor mouse cell nuclei within heterokaryons. Black scale bar: 20 μm.

Figure 1

Click here to download Figure: Fig 1.ppt

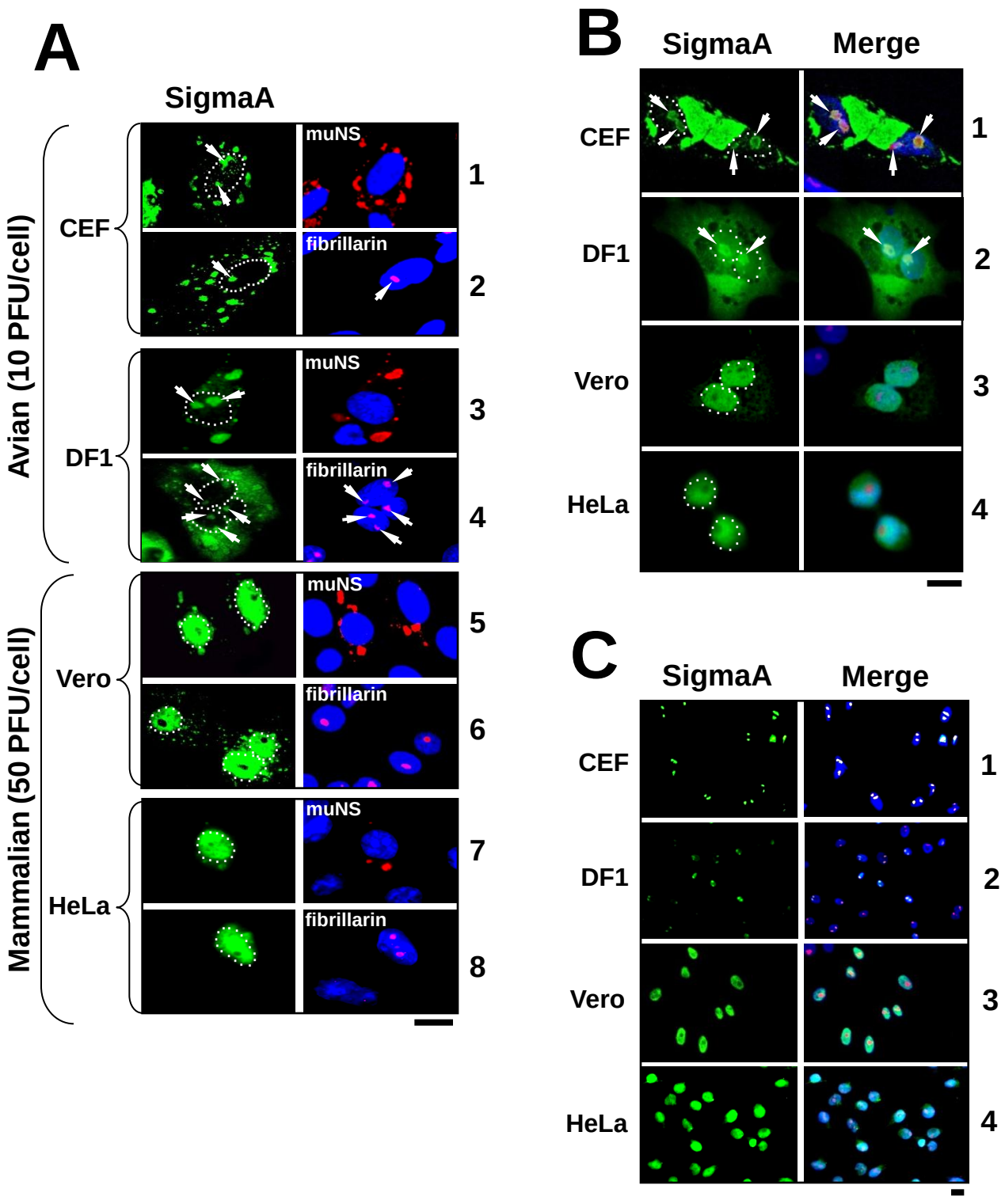

Figure 2

Click here to download Figure: Fig 2.pptx

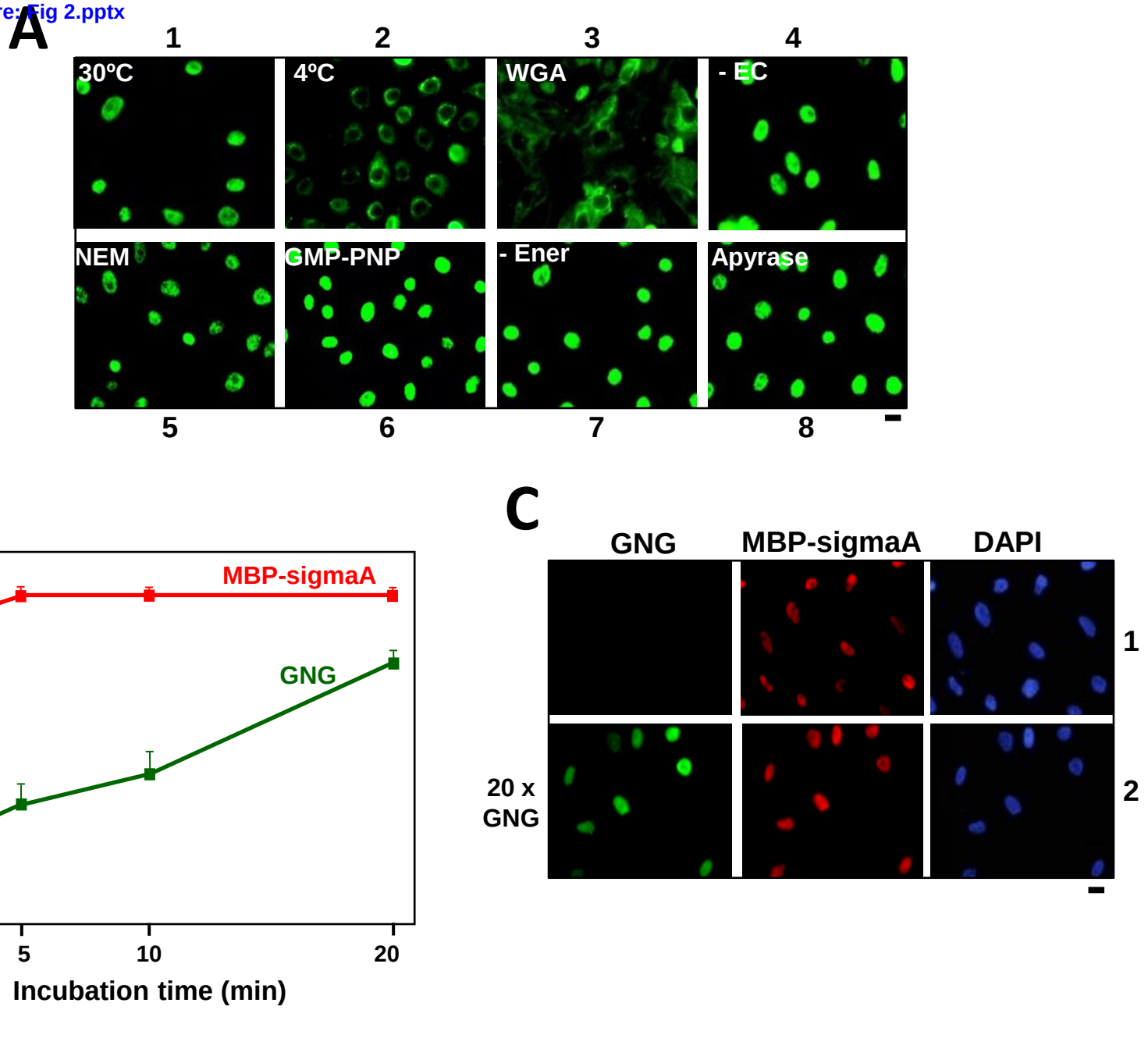

Figure 3

Click here to download Figure: Fig 3.ppt

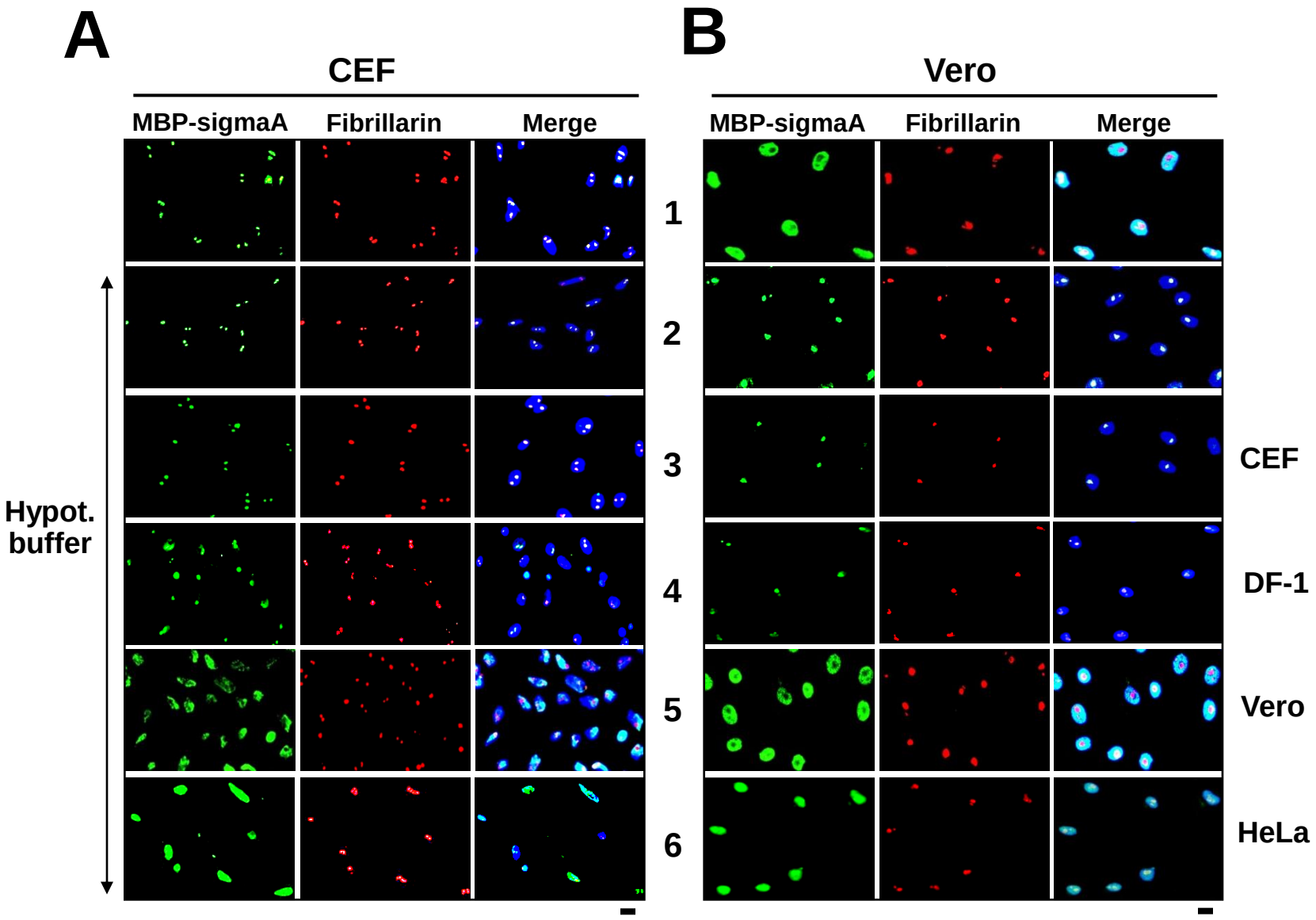

Figure 4

Click here to download Figure: Fig 4.ppt

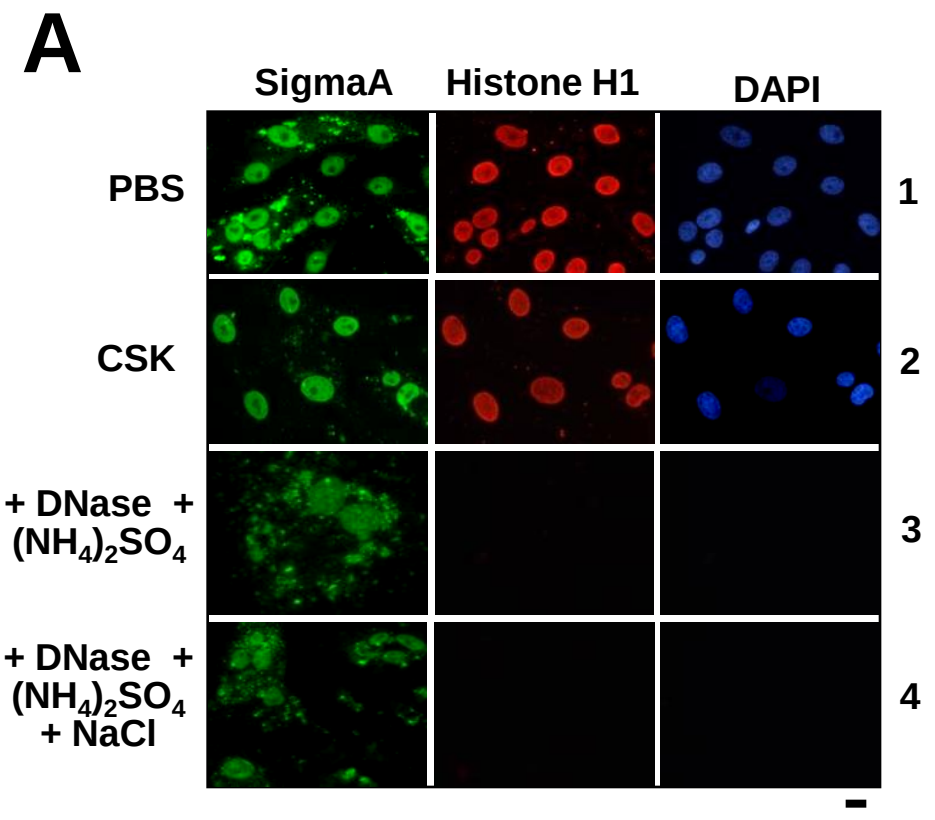

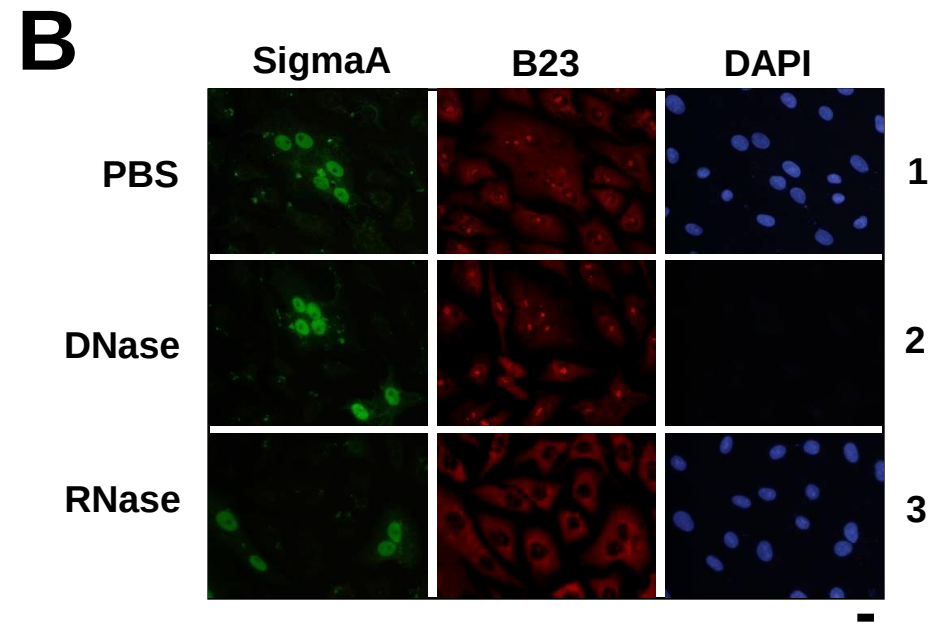

Figure 5
Click here to download Figure: Fig 5.pptx

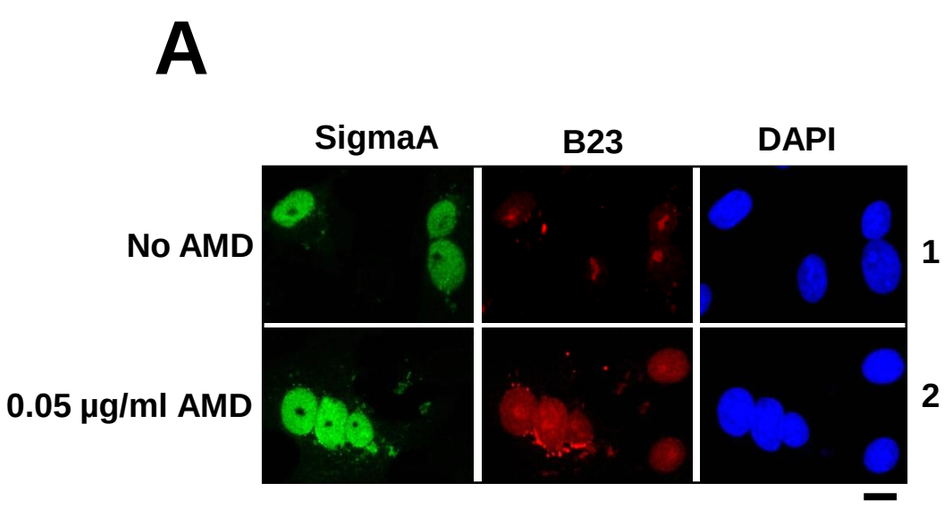

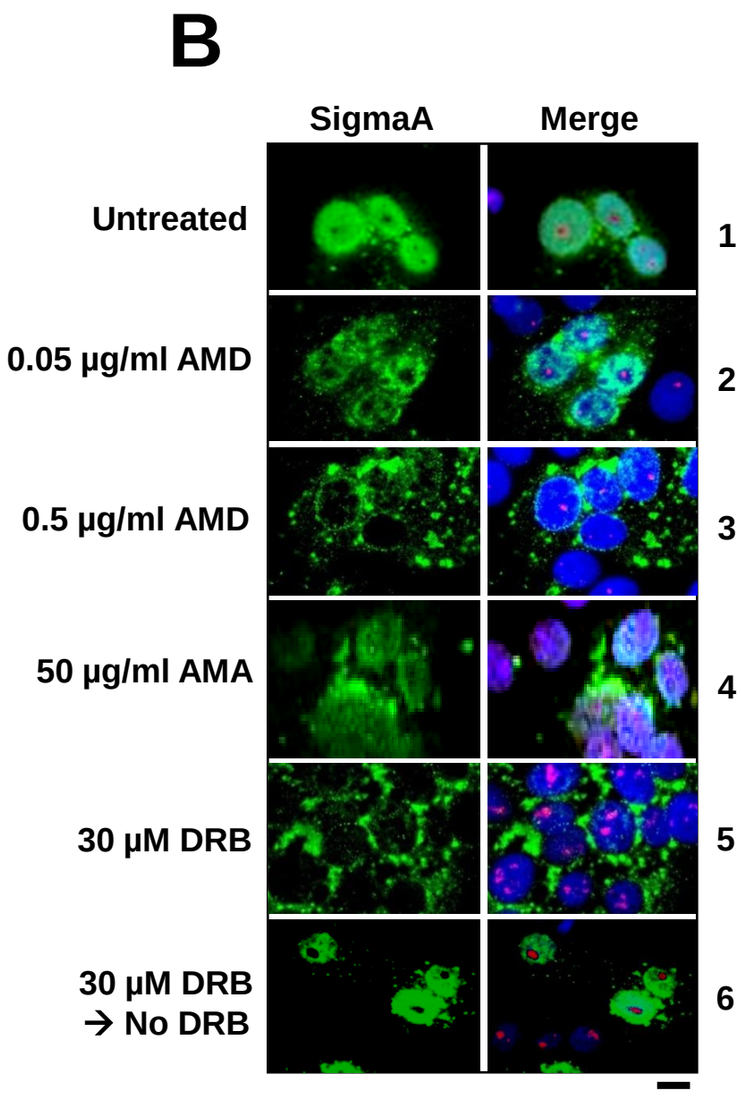

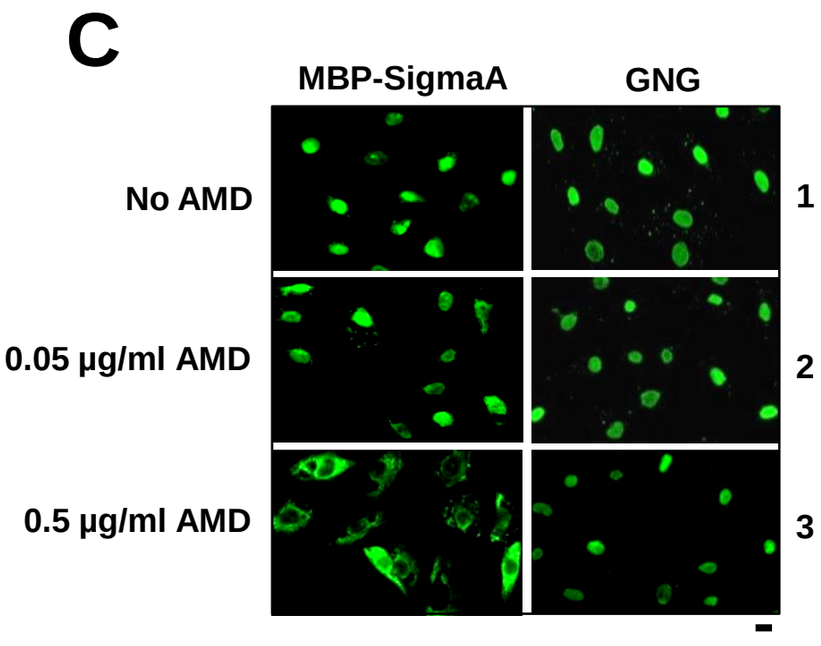

Figure 5

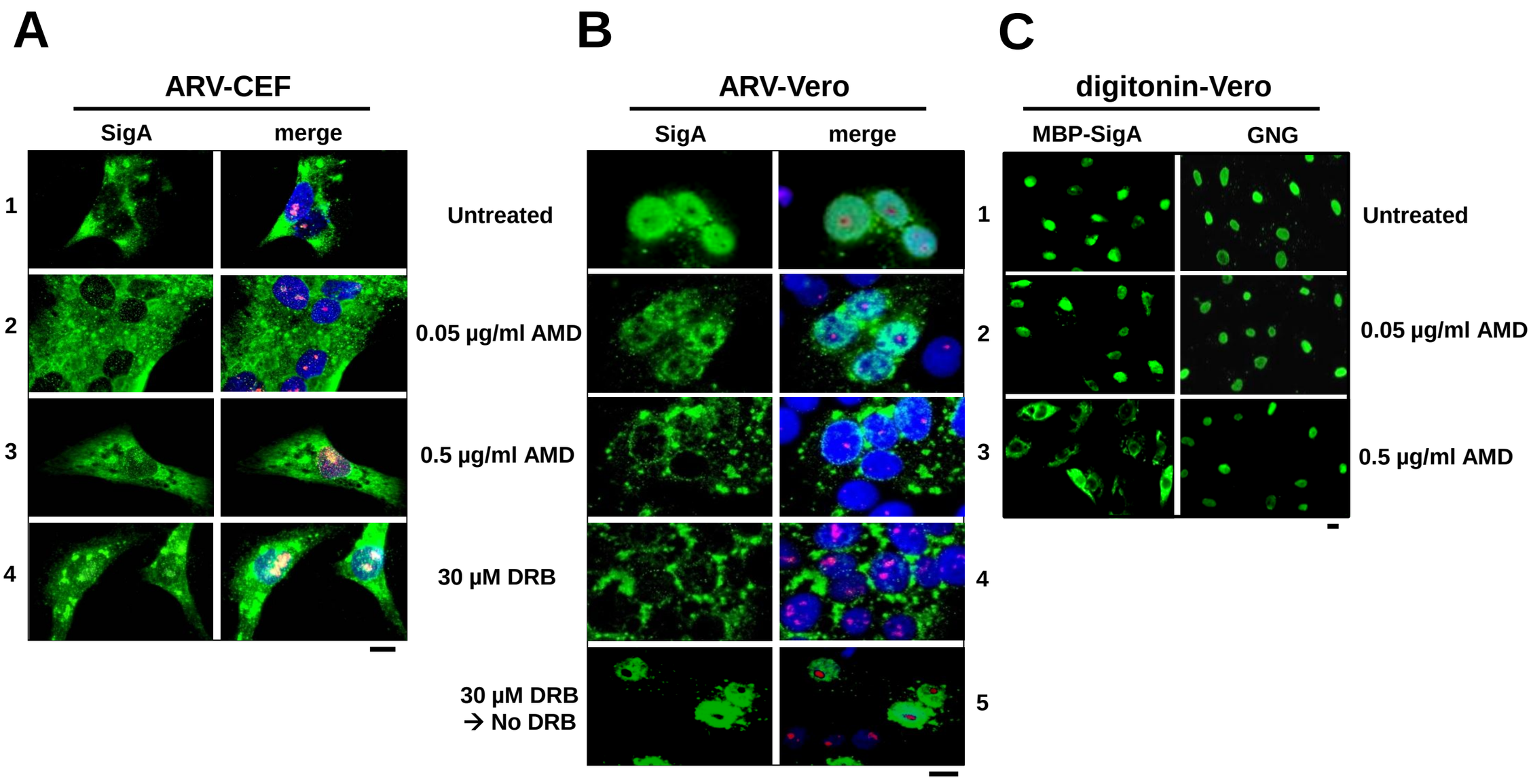
A
ARV-CEF
SigA
merge
1
2
3
4
Untreated
0.05 µg/ml AMD
0.5 µg/ml AMD
30 µM DRB
B
ARV-Vero
SigA
merge
30 µM DRB
→ No DRB
5
C
digitonin-Vero
MBP-SigA
GNG
1
2
3
4
Untreated
0.05 µg/ml AMD
0.5 µg/ml AMD

Figure 6

Click here to download Figure: Fig 6.ppt

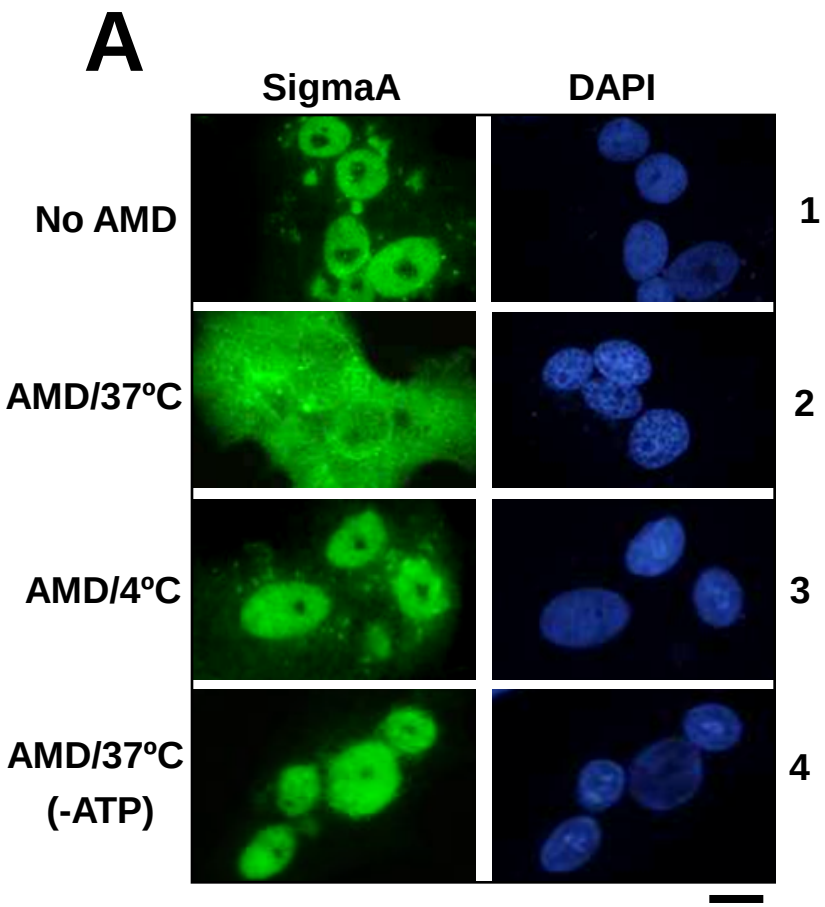

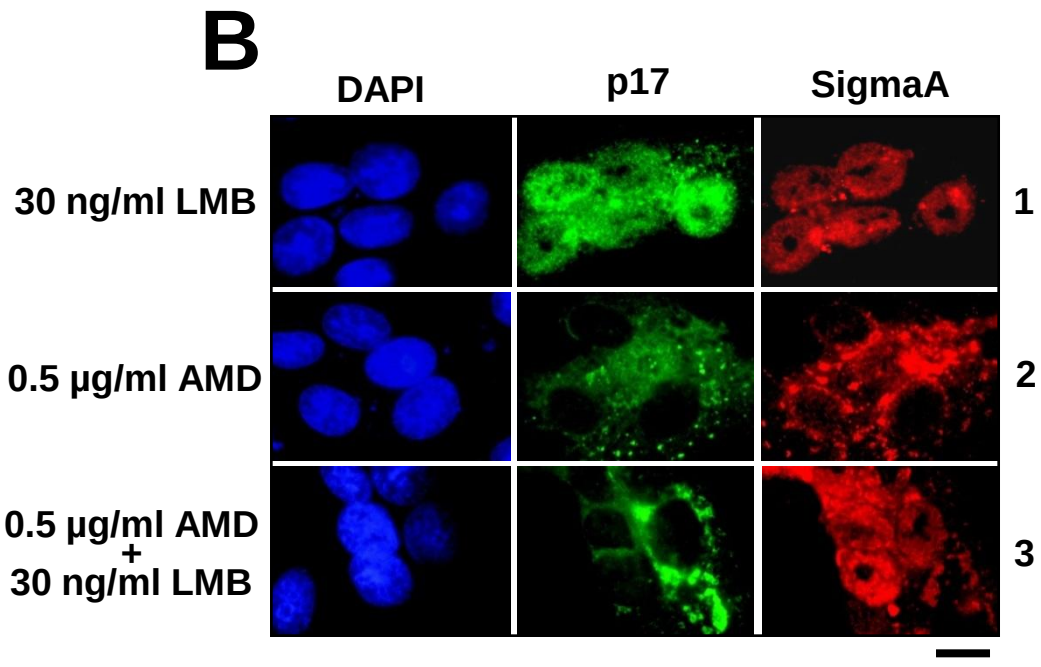

Figure 7

Click here to download Figure: Fig 7.ppt